 https://doi.org/10.3311/PPci.17238

Periodica Polytechnica Civil Engineering, 66(3), pp. 866–875, 2022

A New Approach to the Optimal Placement of the Viscous Damper Based on the Static Force Distribution Pattern

Mohammad Reza Hashemi[1], Reza Vahdani[1*], Mohsen Gerami[1], Ali Kheyroddin[1]

[1] School of Engineering, Semnan University, 35131-19111 Semnan, Iran
[*] Corresponding author, e-mail: rvahdani@semnan.ac.ir

Received: 21 September 2021, Accepted: 08 March 2022, Published online: 16 May 2022

Abstract

Viscous dampers (VDs) are currently used an effective earthquake risk reduction measure. Due to the high cost of this type of dampers, an optimal damper layout across the stories will specifically improve the seismic response and reduce building costs. This paper introduces a new simple three-stage method to determine the optimal placement of VDs on different stories of reinforced concrete structures. In the first stage, the damping demand of each story was determined using the distribution pattern of earthquake forces by the equivalent static method and the story velocity obtained through time-history analysis. In the second stage, the number of dampers required for the structure was calculated, and the location and damping percentage of dampers were precisely determined through an iterative process in the third stage. An indicator representing all basic structural responses was used to evaluate the multiple choices for the damper layout. This process was evaluated for 4, 8 story concrete frames under a near-field earthquake. The results indicated the efficiency of the proposed method in determining the location and damping of VDs on different stories of the structure.

Keywords

viscous damper, near-field earthquake, three-stage algorithm, optimal layout, equivalent static method

1 Introduction

Based on the available seismic regulations, most densely populated areas in the world are located in regions with relatively high and very high seismic risks. It is therefore necessary to use proper energy dissipators in designing new buildings or retrofitting existing buildings. Due to formation of local plastic hinges in various structural points during severe earthquakes, buildings experience large displacements leading to an increased ductility and energy dissipation capacity of the structure. The earthquake energy is therefore dissipated through local damages to the lateral resisting system of the structure. As a reasonable approach, energy dissipators can be used to prevent local structural damages. Dampers are known as one of the most widely used tools for dissipating energy and retrofitting various types of structures. Recently, scholars and engineers have come to this conclusion that dampers are good choices for reducing the seismic structural response against strong ground motions. In the meantime, VDs are widely used due to a very high energy dissipation capacity, a fat hysteresis loop, and easy installation. VDs cause a significant increase in the equivalent structural damping while reducing the overall structural displacement. Hence, VDs could be a very good choice for retrofitting various types of structures. Sugano et al. [1] tested braced concrete frames retrofitted with masonry and concrete frames to evaluate the effect of the resisting system on the improved in-plane strength and ductility of frames. There has been recently a great interest in VDs for retrofitting buildings. Accordingly, numerous studies have been conducted on the effect of VDs on retrofitting of buildings. For instance, Uriz and Whittaker [2] used VDs for retrofitting a steel moment frame after the Northridge Earthquake. In another study, Carden et al. [3] found that VDs are able to cover a more effective hysteretic damping in near-fault earthquakes and thus can be used for structural isolation. Hwang et al. [4] studied the behavior of concrete buildings equipped with VDs and light reinforced concrete walls on the earthquake shaking table. According to their results, the use of dampers in the knee bracing could be an effective retrofitting mechanism at small relative displacements. According to the results of this study, Hwang et al. [5, 6] used the VDs for retrofitting microelectronics factories. Moreover, new

Cite this article as: Hashemi, M. R., Vahdani, R., Gerami, M., Kheyroddin, A. "A New Approach to the Optimal Placement of the Viscous Damper Based on the Static Force Distribution Pattern", Periodica Polytechnica Civil Engineering, 66(3), pp. 866–875, 2022. https://doi.org/10.3311/PPci.17238

design guidelines with a correct procedure for these energy dissipators were provided to improve the performance of VDs in medium- and high-rise buildings. Using the results obtained from the earthquake shaking table, Lin et al. [7] confirmed the high energy dissipation capacity of nonlinear VDs in displacement-based designed buildings and retrofitting existing buildings. Despite multiple advantages of VDs, it is not economically feasible to install this type of dampers at all heights. Consequently, numerous studies have been conducted on the optimal number of dampers at different heights. Takewaki [8] proposed a method for determining the optimal placement of dampers by minimizing the overall displacement of stories on the basis of the displacement transfer function based on the natural frequency of the undamped structure. In fact, all these methods aim at determining the optimal placement and distribution of dampers to reduce the structural displacement. A method was proposed for determining the optimal placement and size of VDs using the genetic algorithm (GA), Kargahi and Ekwueme [9]. The results of this method were comparable with those of other existing methods. Apostolakis and Dargush [10] investigated the optimal design of moment frame systems equipped with damper and bracing assuming the sliding force of the damper as the optimization variable. The genetic algorithm (GA) was used to solve the optimization problem, and the seismic response of stories was evaluated using the square root of the sum of story acceleration. Shin and Singh [11] proposed a method for determining the optimal location of VDs in structures to provide a life safety structural performance level with a minimum structural damage. The GA was used for optimization at three different danger levels. The results showed a significant reduction in the size of objective functions at all danger levels. George et al. [12] studied the nonlinear behavior of VD-equipped structures against near-field earthquakes. A simple effective method was proposed for estimating the damping force using the nonlinear velocity. Landi [13] examined the effect of vertical distribution of damping coefficients of nonlinear VDs on seismic retrofitting of multi-story reinforced concrete frames. Two energy methods and simplified sequential searching algorithms were used for determining the optimal distribution, and the results were compared. The energy methods provided good results in terms of reduced costs, distribution efficiency, and ease of use in comparison with more effective, but more complex methods. Landi [14] studied application of simplified probabilistic methods for seismic evaluation of nonlinear structures equipped with nonlinear VDs. This study aimed at investigating the correlation between the results obtained from the probabilistic method for structures with and without dampers. Banazadeh and Ghanbari [15] evaluated the seismic performance of steel moment frames equipped with nonlinear VDs with a same damping ratio. Their results showed the improved performance of medium steel moment frames using nonlinear VDs, and a significant reduction in the damage probability of this type of structures in comparison with conventional moment frames. The moment frames with a moderate ductility outperformed the conventional moment frames in terms of damage performance. Naderpour et al. [16] evaluated and controlled concrete structures exposed to near-field earthquakes using mass dampers. Their results showed that adding mass dampers on the top story significantly reduced the structural seismic responses depending on the earthquake intensity and seismic zone.

The literature shows the capability of VDs in seismic rehabilitation of steel structures. It is therefore necessary to evaluate the capability of this type of dampers in rehabilitating concrete frames because of slight ductility and in most cases the lack of ductility and limited capacity of concrete structures in absorbing the seismic energy. Given the high energy absorption capacity and other advantages of VDs, a solution should be proposed to use VDs for rehabilitation of concrete structures. Considering the relatively high cost of this type of dampers, a method should be used for optimal placement of VDs on different stories to achieve the best nonlinear structural performance using the least number of VDs. In this study, the optimal location of VDs is determined based on a new pattern for the behavior of concrete structures equipped with dampers under near-field earthquakes. Efforts were also made to determine and evaluate damper location using an index covering all basic structural responses. To this end, 2D 4, 8, story moment frames designed at the DBE danger level based on the static base stress (V) were evaluated.

2 Viscous dampers

Viscous dampers (VDs) cause a significant improvement in the energy dissipation capacity of structures. VDs only cause damping without any change in the structural stiffness (Fig. 1). As a result, the force–displacement diagram of a VD-equipped structure is similar to that for a bare structure. In contrast, the force–displacement relationship for other types of dampers is dependent on environmental conditions, earthquake load intensity, permanent deformations, and bidirectional deformations.

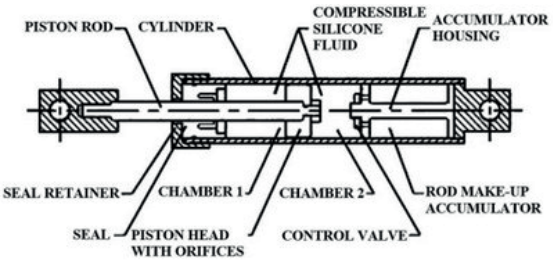

Fig. 1 Details of viscose damper

The resistant force generated in a VD is in an opposite phase to that induced by the structural stiffness. A vibrating structure may be considered to explain this phase difference. When the structure is in its original position, both the structural displacement and the related stiffness force equal zero. At the same time, the structure is moving from its original position with the maximum velocity, and the VD subsequently reacts with the maximum force Fig. 2. The velocity approaches zero as the structure moves further away from its original position. Therefore, the damper reacts with a force of 0 when the structure experiences the maximum displacement and related spring force. Accordingly, both damping and stiffness resisting forces are considered equal in this study.

The energy dissipated by the damper at the *i*th story under the harmonic cycle and the main frequency is expressed as follows [17]:

$$E_{Di} = \pi c \frac{2\pi}{T} \phi_{ij}^2 \cos_{\theta_j}^2 = \frac{2\pi^2 c \phi_{ij}^2 \cos_{\theta_j}^2}{T} . \quad (1)$$

In Eq. (1), c represents viscous damping, T the natural period of the structure, ϕ_{ij} the displacement of both ends of the damper, and θ_j denotes the deviation angle of the damper on the *i*th story.

Therefore, the effective damping of the structure (β_{eff}) is expressed based on the ratio of the energy dissipated by the damper to that applied to the structure in a hysteretic cycle:

$$\beta_{eff} = \beta + \frac{T \sum_j C_j \cos_{\theta_j}^2 \phi_{ij}^2}{4\pi \sum_i M_i \phi_i^2} . \quad (2)$$

In Eq. (2), θ_j represents the deviation angle of the damper on the *i*th story, ϕ_{ij} the displacement of both ends of the damper in the first oscillation mode in the horizontal direction, and Mi shows the seismic weight of each story. The intrinsic damping of the structure (β) is considered to be 5%. Various VD arrangements are used in structures. VDs are connected to the structure in buildings using diagonal or chevron bracing. Due to limitations regarding installation of dampers by above methods in buildings and considering their severe responses to ground motions under near-field earthquakes (with a relatively high frequency), a new control system should be designed to overcome these severe responses. In this study, various stories in the building structures are assumed to be connected to a free rigid wall outside the building using VDs Fig. 3.

Hence, Eq. (2) is rewritten as follows for the damper layout on stories:

$$\beta_{eff} = \beta + \frac{T \sum_j C_j \phi_{ij}^2}{4\pi \sum_i M_i \phi_i^2} . \quad (3)$$

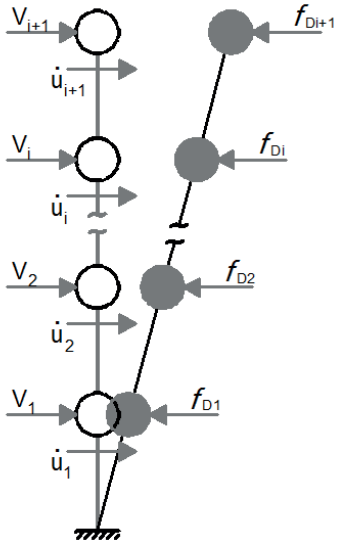

Fig. 2 The force of dampers on the structural floors

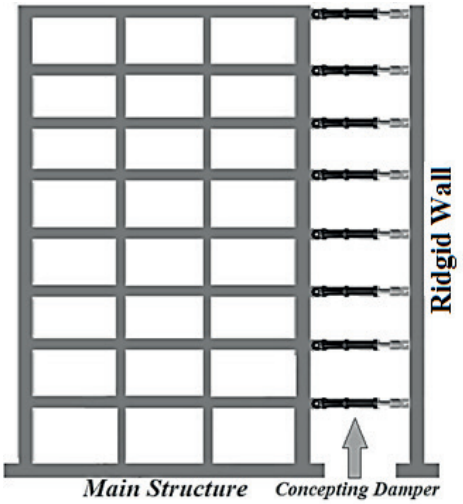

Fig. 3 Connect the viscose damper to the rigid wall

VDs improve the structural damping without any change in the structural stiffness. This eventually leads to reduced acceleration of stories and the force exerted on both structural and non-structural elements. The presence of a free rigid solid does not cause any change in the structural stiffness, and damping can be distributed on various stories according to the story mass. A damage suspected in structural elements would lead to changes in structural characteristics including structural stiffness and structural frequency. Such variations would, in turn, result in the creation of a new strain energy level in the damaged structure.

3 A new approach to damping distribution on stories

3.1 Damping distribution based on shear force and story velocity

In the equivalent static method, the earthquake-induced lateral force (V) is calculated from Eq. (4). The base shear in this method is selected in such a way that the maximum structural deformation would be consistent with that predicted at the intended danger level. If the structure behaves linearly under the applied forces, the forces obtained for the structural elements will be close to those predicted during the earthquake. However, if the structure enters the nonlinear phase, the forces calculated by this method will be less than those applied to the structure [17]:

$$V = C_1 C_2 C_m S_a W . \tag{4}$$

In Eq. (4), C_1 represents the correction factor for the non-vibrational displacements of the system, C_2 the correction factor for the effect of reduced stiffness and strength of structural elements on the displacement induced by the cyclic deterioration, C_m the effective mass coefficient to apply the effect of higher modes, S_a the spectral acceleration in the interval T, and W shows the effective seismic weight of the structure. The shear base distribution pattern obtained from the equivalent static method (V) at the structure height is as follows:

$$F_x = C_{vx} V, \; C_{vx} = \frac{w_x h_x^k}{\sum_{i=1}^{n} w_i h_i^k}, \; k = 0.5T + 0.75 . \tag{5}$$

In Eq. (5), F_x is the lateral force at the level of the story x, C_{yx} the distribution coefficient of the lateral force at the structure height, h_x the height of the story x, and w_i shows the seismic weight of each story. The shear force in each story (V_i) is obtained by adding the lateral force of that story to that of upper stories.

Assuming linear VDs, the damping force is obtained from Eq. (6):

$$f_D = C \,\mathrm{sgn}(\dot{u}) |\dot{u}|^{\alpha}, \; \alpha = 1 \Rightarrow f_D = -C\dot{u} . \tag{6}$$

In Eq. (6), f_p and u, respectively represent the damping force and damper velocity. If the dampers are installed on all stories as shown in Fig. 4, the damping of each story is obtained from Eq. (7) by equating the shear force on each story (V_i) with Eq. (6):

$$f_D \approx V \Rightarrow C\dot{u} = V \Rightarrow C_i = \frac{V_i}{\dot{u}_i} . \tag{7}$$

In Eq. (7), V_i and u_i, respectively represent the shear force on the ith story and the relative velocity of both ends of the damper on the i^{th} story, which is assumed equal to the velocity of the i^{th} story ($FD_i = FS_i$).

Accordingly, the damping coefficient of the VD relative to the shear force in each story can be expressed as follows Eq. (8):

$$C_i = \lambda V_i . \tag{8}$$

In Eq. (8), λ represents the coefficient of proportionality. Using the above equation, the overall damping coefficient as the sum of damping coefficients for all stories can be rewritten as follows Eq. (9):

$$\sum_i C_i = \lambda \sum_i V_i \Rightarrow \lambda = \frac{\sum_i C_i}{\sum_i V_i} . \tag{9}$$

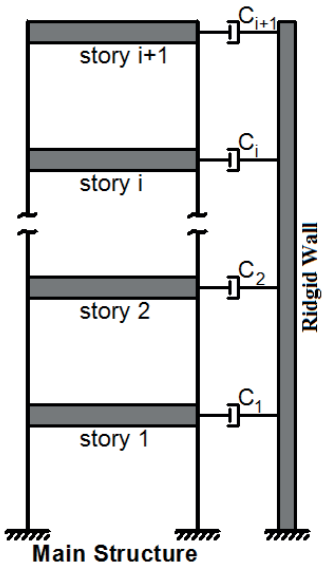

Fig. 4 Viscous damper placement in the floors

By inserting Eq. (9) in Eq. (8), the damping coefficient of the VD on each story is obtained Eq. (10).

$$C_i = \frac{V_i}{\sum_i V_i} . \sum_i C_i \tag{10}$$

The damping distribution on the stories is similar to that of the lateral earthquake loading as shown in Fig. 5.

3.2 Problem formulation for determining the number and optimal placement of VDs across different stories

The uniform deformation theory (UDT) can be a key factor in determining the optimal pattern of damping distribution in nonlinear damped structures to show the best behavior against dynamic loads. On the other hand, all methods used for the optimal design of structures fail in the nonlinear range or need nonlinear dynamic analyses, and thus cannot be employed for this purpose. At the same time, some structural elements may not still reach the allowable ductility, and the full capacity of energy dissipators may not be employed. Accordingly, considering the UDT-based iterative process to achieve an optimal structure, the energy dissipation elements should be arranged to achieve the minimum structural responses (e.g., drift, acceleration, velocity,…). In other words, in those structural points where the responses are in the allowable range, damping decreases and is added to the other points. To this end, the changes should be applied gradually in the iterative process to achieve a proper convergence. Structural damping distribution may be influenced by load distribution. Hence, the structural seismic performance can be improved by choosing a correct pattern for the optimal damper distribution. In general, the damper performance is influenced by multiple indicators such as the reduced absolute structural acceleration, reduced shear base, reduced relative displacements, increased energy dissipation, reduced maximum strain energy, and the total area under the strain energy curve. The ratio of the damper-equipped frame to the original moment frame is considered in all these dimensionless indicators. VDs not only reduce the structural displacements, but cause a decrease in the forces exerted to the structure and thereby acceleration of stories without any increase in the structural stiffness. As a result, to find the optimal layout, the major responses reduced by VDs should be considered individually or in combination. The following function is defined to consider the simultaneous effect of the most important responses (drift and acceleration of stories) on the optimal distribution pattern:

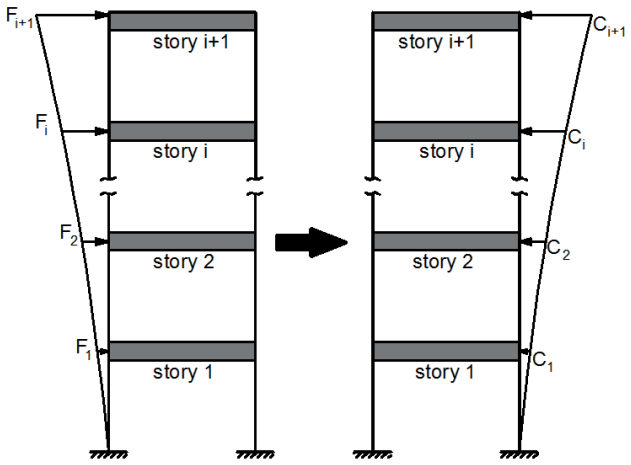

Fig. 5 Damping distribution pattern based on static loading pattern

$$RPI = \alpha . \frac{Drift_{Damped}}{Drift_{MRF}} + \beta . \frac{\mathrm{Re}\,sDrift_{Damped}}{\mathrm{Re}\,sDrift_{MRF}} + \gamma . \frac{RMSAcc_{Damped}}{RMSAcc_{MRF}} + \delta . \frac{MaxAcc_{Damped}}{MaxAcc_{MRF}} \tag{11}$$

In Eq. (11), the sum of the weights α, β, γ, and δ equals unity, $Drift_{Damped}$ and $Drift_{MRF}$, respectively show the maximum drifts of stories with and without a damper, and $MaxAcc_{Damped}$ and $MaxAcc_{MRF}$, respectively represent the maximum accelerations of stories with and without a damper. The index RPI includes the key structural response components during the earthquake and is able to evaluate the effect of VD layouts on different stories. On the other hand, the performance of this index can be improved by choosing appropriate weight coefficients for its different parameters.

$$\mathrm{Re}\,sDrift = \max\left(\frac{\left| D_{i(T_D)} - D_{i-1(T_D)} \right|}{h_i} \right) \tag{12}$$

for $i = 1,\ldots,N_{story}$

Res$Drift_{Damped}$ and Res$Drift_{MRF}$ obtained from Eq. (12), respectively represent the maximum residual drifts on the stories with and without the damper:

In Eq. (12), $D_{i(T_D)}$ and $D_{i-1(T_D)}$ respectively show the deformation of the ith and $(i-1)^{\text{th}}$ stories during the earthquake. $RMSAcc_{Damped}$ and $RMSAcc_{MRF}$ obtained from Eq. (13), respectively represent the maximum accelerations of stories with and without the damper:

$$RMSAcc = \max\left(\sqrt{\sum_{j=1}^{N} \left(Acc_i(t_j) \right)^2 / N} \right) \tag{13}$$

for $i = 1,\ldots,N_{story}$.

In Eq. (13), $Acc_i(t_j)$ and N, respectively denote the absolute acceleration of the i^{th} story in the interval j and the number of time steps of the earthquake. In this study, the optimal placement of dampers across the stories is obtained based on an iterative process. The structural response in this iterative process should be in such a way that the index RPI approaches its minimum value. In other words, locating is performed to minimize the objective function. Eq. (11) shows the objective function for determining the optimal placement of VDs across the stories. Using this equation, the iterative process is defined to achieve the damping coefficients of dampers on various stories to obtain a reasonable seismic performance. Accordingly, the iterative process is formulated as follows:

$$\begin{aligned} &Find: C^T = \{C_1, C_2, \ldots, C_n\} \\ &Minimize: F = minimize(RPI). \end{aligned} \tag{14}$$

In Eq. (14), n represents the number of stories.

3.3 The procedure for determining damping and optimal location of dampers across different stories

An iterative process based on the combination of various structural responses is used in this paper for determining the correct distribution of dampers to improve the structural performance and achieve an optimal layout.

a. The design of structures based on the DBE design earthquake and ACI 318-14 Code [18].
b. Determination of damping percentage of each story from Eq. (6).
c. Calculation of the overall damping demand by summing the damping obtained for different stories in the previous stage (Eq. 6).
d. The initial damping distribution at the story level from Eq. (9).
e. Determination of the number of dampers required using an iterative process in which the first damper with the damping percentage obtained in the Stage d is placed on the top story, and the index RPI is determined through the nonlinear time-history analysis of the structure based on the recorded near-field earthquakes. If the index RPI exceeds beyond the intended range, the next damper is added to the next story, and this iterative process is repeated to achieve the minimum RPI.
f. Controlling the damping percentage added to the structure to not exceed that specified in the relevant codes.
g. The sensitivity analysis of the index RPI to the displacement of dampers determined in the Stage f.

To this end, all possible damper layouts across the stories should be evaluated. For this purpose, the number of dampers obtained in the Stage e is located randomly on various stories based on a continuous distribution. For each damper arrangement, the objective function, RPI, is determined through the nonlinear time-history analysis of the structure under different earthquake stimuli. The iterations stop if the index RPI and the damping percentage are placed in the allowable ranges. Otherwise, the iterative process algorithm is repeated to determine the optimal damping and layout of dampers. By repeating the above steps, the algorithm eventually converges, and the optimal distribution of dampers is obtained on different Stories. Fig. 6 shows the iterative process flowchart for determining the location and damping percentage of dampers at the best structural performance level.

4 Numerical examples

To investigate the efficiency of the proposed method, the method mentioned in reference [19] as the standard insertion method was used for comparison in this research. In this method, damping is distributed proportionate to the stiffness throughout the structure. Uniform damping might be the most appropriate method of insertion of damper, but maybe is not the most effective. Thus, this method allocates the total uniform damping to each floor equally as the share of each floor is equal to the ratio of the total damping Ct over the number of stories.

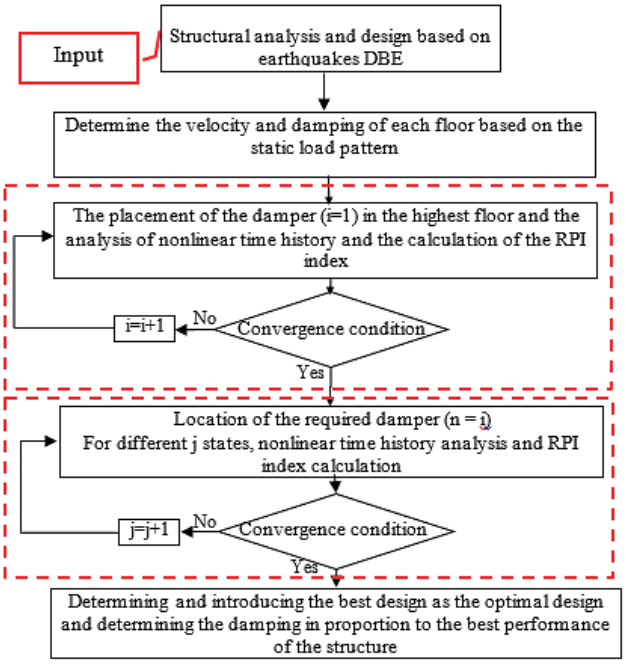

Fig. 6 Flowchart is the iterative process the positioning and optimal damping of the damper

In this study, 4- and 8-story concrete moment frames were investigated. Residential buildings and Type III soil were considered in a high-seismic risk. The Iranian Seismic Code (Standard No. 2800) was used to determine the earthquake-induced forces [20]. The modulus of elasticity (E) and density (ρ) for all concrete members were considered to be 26517.5 MPa and 2500 kg/m^3, respectively. The overall height of stories in all three frames was 3.6 m. The linear distributed dead and live loads of 2000 and 600 kg/m were applied, respectively. C25 concrete was used in the beam and columns, and AIII reinforcement was employed. The optimal location of dampers in the concrete frames was obtained with the help of Opensees and MATLAB. In all numerical examples, α, β, γ, and δ were equal to 1.3, 1.3, 1.6, and 1.6, respectively.

4.1 Accelerograms

The structural response to earthquakes is dependent on the specifications of accelerograms applied such as the frequency content and maximum acceleration. On the other hand, the structural response may be affected by the soil type used for recording the accelerogram and the distance of the recording site from the fault. A set of near-fault earthquake accelerograms was used in this study. To this end, 10 earthquake records with different PGAs were used. Table 1 presents the accelerogram specifications.

4.2 The 4-story concrete frame

To evaluate the effect of VD layout on the structural performance, a 4-story concrete frame was examiend as the first numerical example Fig. 7.

The velocity of stories was calculated through the nonlinear time-history analysis. Fig. 8 shows the initial damping distribution pattern across the stories determined from Eq. (10). At this stage, the number of stories on which the VDs should be installed is determined based on the resulting damping pattern. According to the results in Table 2, only one damper was determined by the algorithm as the numebr of energy dissipators required for the structure. In the next step, the optimal location and the damping demand are obtained through locating dampers across the stories with different damping levels. Table 2 shows the optimal location of dampers and required damping. As shown in Table 2, the algorithm achieved the best response by locating the damper on the 3rd story. Figs. 8 to 10 show the results obtained from the damper layout determination by the algorithm.

According to the results, by locating the damper on the 3th story, the drift, acceleration of stories were significantly reduced, and the index RPI reached 0.34 after 4 iterations as shown in Fig. 10. By locating the dampers and assigning the structural damping percentage, the structural damping increased by 31%, which is less than the allowable damping percentage of 35%.

Table 1 Near-field accelerometers used in structural analysis

NO	Earthquake	Year	Magnitude	PGA(g)
1	Turkey	2003	6.5	0.1
2	manjil	2003	4.4	0.13
3	ChiChi-chy065	2017	7.3	0.6
4	ChiChi-tap95-1	2017	4.4	0.15
5	Imperial valley	2005	6.5	0.24
6	Kobe-hik	1978	6.4	0.14
7	Northridge	1981	5.9	0.1
8	Imperial valley-outers	1981	5.9	0.26
9	Lomaprieta	1981	5.9	0.23
10	Tabas	1981	5.9	0.1

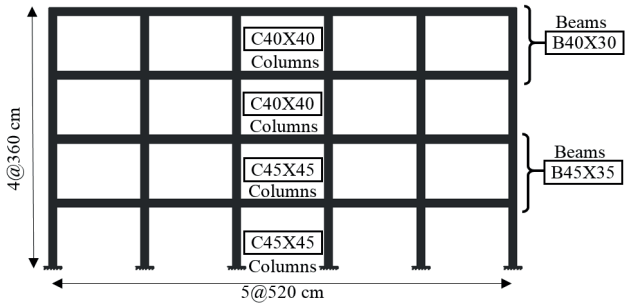

Fig. 7 4-story concrete frame

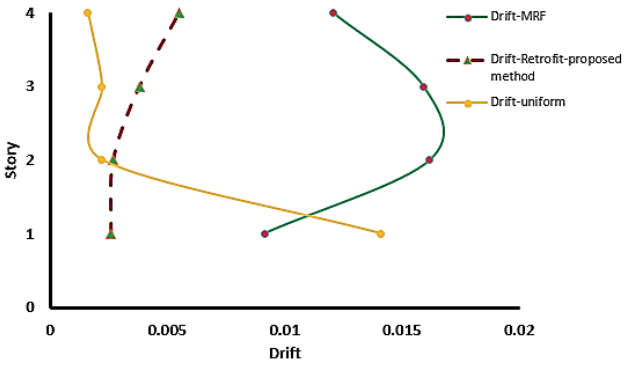

Fig. 8 Drift the floors with the damper on the third floor

Table 2 The position and damping required of the structure

Story No	Damping (KN.S/MM)
1	0
2	0
3	26.00957
4	0

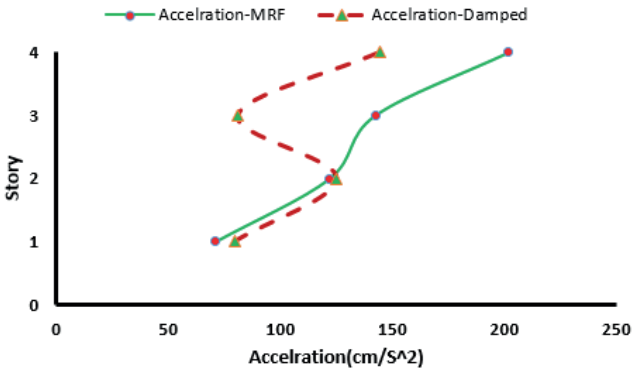

Fig. 9 Acceleration the floors with the damper on the third floor

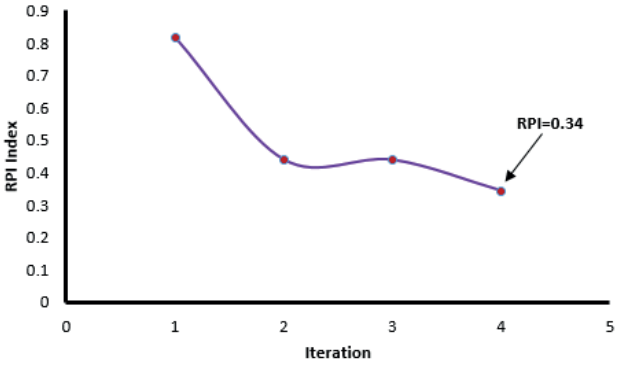

Fig. 10 RPI convergence

4.3 The 8-story concrete frame

An 8-story concrete moment frame Fig. 11 was examined to evalaue the effficieny of the proposed metod. The 8-story frame was analyzed and designed under the DBE earthquake. According to FEMA356 Code, a maximum effective damping (βeff) of 35% was considered.

An 8-story concrete moment frame Fig. 11 was examined to evalaue the effficieny of the proposed metod. The 8-story frame was analyzed and designed under the DBE earthquake. According to FEMA356 Code [17], a maximum effective damping (β_{eff}) of 35% was considered. The damping obtained from the proposed method should not exceed this value. The damping coefficients of the damper on various stories were calculated from Eq. (10), and the results are shown in Table 3. Using the proposed algorithm and based on the resulting damping, the number of stories requiring VDs to minimize the index RPI was specified. According to the output of the first stage, the structrue needs only three dampers to reduce the index RPI. The exact location and damping level should be therefore determined based on the number of dampers. The exact location and damping intensity reported in Table 3 were obtained by implementing the second step of the algorithm through different placements of dampers. As seen in Table 3, the damper was located on the three upper stories based on the damping obtained from the static lateral load. Figs. 12 to 14, respectively show the drift, acceleration, and RPI of stories when the damper is placed on the three upper stories of the structure.

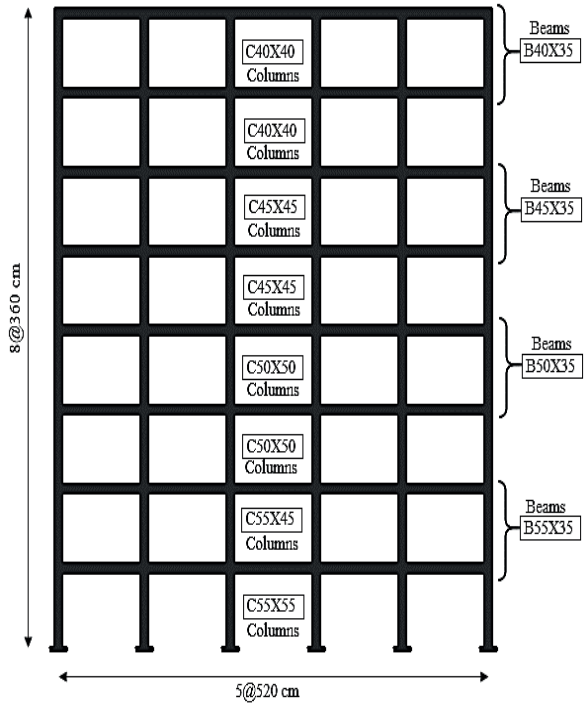

Fig. 11 8-story concrete frame

Table 3 The position and damping required of the structure

Story No	Damping (KN.S/MM)
1	0.0
2	0.0
3	0.0
4	0.0
5	0.0
6	45.478
7	47.868
8	48.875

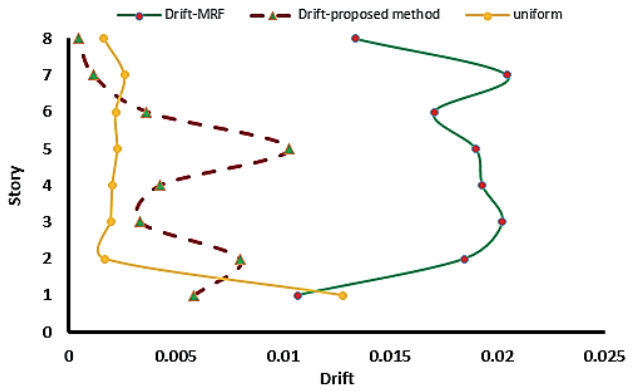

Fig. 12 Drift the floors with the damper on the third floor

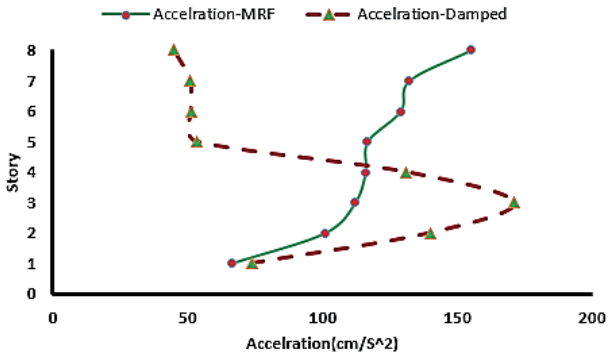

Fig. 13 Acceleration the floors with the damper on the third floor

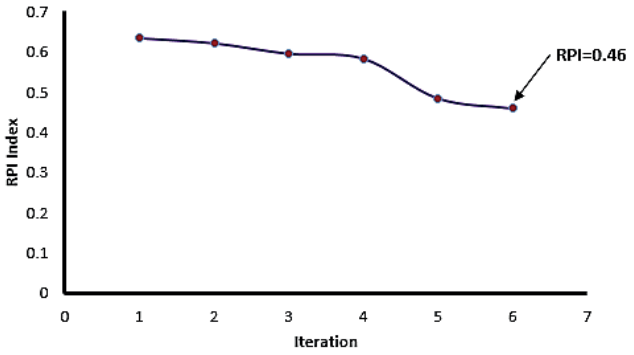

Fig. 14 RPI convergence

Fig. 14 shows the convergence of the index RPI. According to the results, the damping obtained from the static load pattern and the layout of dampers cause a significant reduction in the drift of stories. The results also show the superiority of the proposed method over other existing methods for determining the optimal damping layout and structural damping so that other methods obtain the optimal layout and damping based on the uniform distribution pattern. The structral damping obtained from this layout equals 31%, which is in a reasonable range as compared to its allowable value.

5 Conclusions

A new approach was studied to determine the optimal number and layout of VDs. To this end, a three-stage method was used to determine the optimal number and layout of dampers. Accordingly, an index was introduced to consider the simultaneous effect of all basic structural responses based on the drift and acceleration of stories. Based on this index, the number of required dampers was first determined. The location and damping percentage of dampers were obtained in the second stage through an iterative process. The results showed that the proper damping distribution across the stories based on the static loading pattern causes significant changes in the structural responses so that the damping added to the structure does not exceed its allowable limit. The numerical analysis of three structures showed that dampers are usually located on the upper stories of the structure on the 1/3 to 1/4 stories. On other hand, the effect of dampers installed on the upper stories in reducing the structural displacement is greater than acceleration due to the negative effect of dynamic forces exerted to the structural system by dampers. Increasing the number of dampers negatively affects the acceleration and causes an increase in the acceleration of stories.

The advantages of using this method are as follows:

1. The simplicity of its usage in a way that could be presented in engineering levels.
2. It provides an acceptable estimation of the damping required in the structure for the initial estimation.
3. It does not need nonlinear analyses that mostly are time-consuming; so, the algorithm is of an appropriate speed.
4. The important seismic parameters of the structure such as displacement, velocity and acceleration simultaneously involve in determining the location and level of damping of the dampers.
5. According to the conditions of the structure, the amount of the effect of the seismic parameters (displacement, velocity and acceleration) is adjustable in an index called RPI.

References

[1] Sugano, S. "Study of seismic behavior of retrofitted RC buildings, seismic engineering, research and practice", In: Proceedings of the Sessions Related to Seismic Engineering at Structures Congress, San Francisco, CA, USA, 1989, pp. 517–526. [online] Available at: https://cedb.asce.org/CEDBsearch/record.jsp?dockey=0060438

[2] Uriz, P., Whittaker, A. S. "Retrofit of pre- Northridge steel moment-resisting frames using fluid viscous dampers", The Structural Design of Tall Buildings, 10(5), pp. 371–390, 2001. https://doi.org/10.1002/tal.199

[3] Carden, L. P., Davidson, B. J., Larkin, T. J., Buckle, I. G. "Retrofit of seismically isolated structures for near-field ground motion using additional viscous damping", Bulletin of the New Zealand Society for Earthquake Engineering, 38(2), pp. 106–118, 2005. https://doi.org/10.5459/bnzsee.38.2.106-118

[4] Hwang, J.-S., Kim, H., Kim, J. "Estimation of the modal mass of a structure with a tuned-mass damper using H-infinity optimal model reduction", Engineering Structures, 28(1), pp. 34–42, 2006. https://doi.org/10.1016/j.engstruct.2005.06.022

[5] Hwang, J.-S., Wang, S.-J., Huang, Y.-N. Chen, J.-F. "A seismic retrofit method by connecting viscous dampers for microelectronics factories", Earthquake Engineering Structural Dynamics, 36(11), pp. 1461–1480, 2007.
https://doi.org/10.1002/eqe.689

[6] Hwang, J.-S., Huang, Y.-N., Yi, S.-L., Ho, S.-Y. "Design Formulations for Supplemental Viscous Dampers to Building Structures", Journal of Structural Engineering, 134(1), pp. 22–31, 2008.
https://doi.org/10.1061/(ASCE)0733-9445(2008)134:1(22)

[7] Lin, Y.-Y., Chang, K.-C., Chen, C.-Y. "Direct displacement-based design for seismic retrofit of existing buildings using nonlinear viscous dampers", Bulletin of Earthquake Engineering, 6, pp. 535–552, 2008.
https://doi.org/10.1007/s10518-008-9062-9

[8] Takewaki, I. "Optimal damper placement for planar building frames using transfer functions", Structural and Multidisciplinary Optimization, 20(4), pp. 280–287, 2000.
https://doi.org/10.1007/s001580050158

[9] Kargahi, M., Ekwueme, C. G. "Structural Optimization of Viscous Dampers Using Genetic Algorithms for Improving Seismic Performance of Existing", In: Proceeding of the ATC & SEI 2009 Conference on Improving the Seismic Performance of Existing Buildings and Other Structures, San Francisco, CA, USA, 2009, pp. 955–966.
https://doi.org/10.1061/41084(364)87

[10] Apostolakis, G., Dargush, G. F. "Optimal Seismic Design of Moment Resisting Steel Frames with Hystertic Passive Device", Earthquake Engineering and Structural Dynamics, 39(4), pp. 355–376, 2010.
https://doi.org/10.1002/eqe.944

[11] Shin, H., Singh, M. P. "Minimum failure cost-based energy dissipation system designs for buildings in three seismic regions – Part II: Application to viscous dampers", Engineering Structures, 74(1), pp. 275–282, 2014.
https://doi.org/10.1016/j.engstruct.2014.05.012

[12] George D. H., Nikos, G. P. "Maximum damping forces for structures with viscous dampers under near-source earthquakes", Engineering Structures, 68, pp. 1–13, 2014.
https://doi.org/10.1016/j.engstruct.2014.02.036

[13] Landi, L., Conti, F., Diotallevi, P. P. "Effectiveness of different distributions of viscous damping coefficients for the seismic retrofit of regular and irregular RC frames", Engineering Structures, 100(1), pp. 79–93, 2015.
https://doi.org/10.1016/j.engstruct.2015.05.031

[14] Landi, L., Vorabbi, C., Fabbri, O., Diotallevi, P. P. "Simplified probabilistic seismic assessment of RC frames with added viscous dampers", Soil Dynamics and Earthquake Engineering, 97(1), pp. 277–288, 2017.
https://doi.org/10.1016/j.soildyn.2017.03.003

[15] Banazadeh, M., Ghanbari, A. "“Seismic performance assessment of steel moment-resisting frames equipped with linear and nonlinear fluid viscous dampers with the same damping ratio", Journal of Constructional Steel Research, 136(1), pp. 215–228, 2017.
https://doi.org/10.1016/j.jcsr.2017.05.022

[16] Naderpour, H., Kiani, A., Kheyroddin, A. "Structural control of RC buildings subjected to near-fault ground motions in terms of tuned mass dampers", Scientia Iranica, 27(1), pp. 122–133, 2020.
https://doi.org/10.24200/sci.2018.5600.1365

[17] FEMA-356 "Prestandard and commentary for the seismic rehabilitation of buildings", [pdf] Federal Emergency Management Agency, Washington, DC, USA, 2000. Available at: https://www.nehrp.gov/pdf/fema356.pdf

[18] ACI Committee 318 "Building Code Requirements for Structural Concrete (ACI318-14)", American Concrete Institute, Farmington Hills, MI, USA, 2014.

[19] ASCE "Minimum Design Loads and Associated Criteria for Buildings and Other Structures (ASCE/SEI 7-22)", American Society of Civil Engineers, Reston, VA, USA, 2022. [online] Available at: https://www.asce.org/publications-and-news/asce-7

[20] STD-2800 "Iranian seismic design code for Buildings", Rood, Housing & Urban Development Research Center, Tehran, Iran, 2020.